Article

Synthesis of silver modified bioactive glassy materials with antibacterial properties via facile and low-temperature route

I. Gonzalo-Juan[1,*], F. Xie[1], M. Becker[1], D. U. Tulyaganov[1,2], E. Ionescu[1], S. Lauterbach[3], F. De Angelis Rigotti[4], A. Fischer[4,5], and R. Riedel[1]

[1] Technische Universität Darmstadt, Institut für Materialwissenschaft, Otto-Berndt-Straße 3, D-64287 Darmstadt, Germany
[2] Department of Natural - Mathematical Sciences, Turin Polytechnic University in Tashkent, 17, Small Ring, Tashkent 100095, Uzbekistan
[3] Technische Universität Darmstadt, Institut für Angewandte Geowissenschaften, Schnittspahnstrasse 9, 64287 , Darmstadt, Germany
[4] Division of Vascular Signaling and Cancer (A270), German Cancer Research Center (DKFZ), Im Neuenheimer Feld 280 ,69120 Heidelberg, Germany
[5] Department of Medicine I and Clinical Chemistry, University Hospital of Heidelberg, Heidelberg 69120, Germany

* Correspondence: isabel.gonzalo@tu-darmstadt.de

Abstract: There is an increasing clinical need to develop novel biomaterials that combine regenerative and biocidal properties. In this work, we present the preparation of silver /silica based glassy bioactive (ABG) compositions via a facile, fast (20h), and low temperature (80 °C) approach and their characterization. The fabrication process included the synthesis of the bioactive glass (BG) particles followed by the surface modification of the bioactive glass with silver nanoparticles. The microstructural features of ABG samples before and after exposure to simulated body fluid (SBF) as well as their ion release behavior during SBF test were evaluated using infrared spectrometry (FTIR), ultraviolet- visible (UV-Vis) spectroscopy, X-ray diffraction (XRD), electron microscopies (TEM and SEM) and optical emission spectroscopy (OES). The antibacterial properties of the experimental compositions were tested against Escherichia coli (E. coli). The results indicated that the prepared ABG materials possess antibacterial activity against E. coli, which is directly correlated with the glass surface modification.

Keywords: Bioactive glass; antibacterial; silver; nanocomposites; E. coli; ion release

1. Introduction

One of the main issues connected to orthopaedical surgery are bacterial infections that might lead to implant failure, devastating health complications for the patient, and high treatment costs [1]. van de Belt et al. [2] reported that, when orthopedic implants are in contact with blood, plasma proteins can form a conditioning film on the surface of the implant where microorganisms can easily adhere to. Current efforts are focused on the modification of the surface of bioactive materials with inorganic antibacterial elements to reduce the use of antibiotics and the associated drug resistance issues. Antibacterial properties can be provided to glasses typically by ion exchange either in aqueous solutions or molten salts. Among various inorganic antibacterial agents, silver has been demonstrated as a suitable candidate for ion exchange approach due to its great ability to enter the silicate glass structure. Moreover, it exhibits a broad-spectrum bactericidal behavior at low concentrations without causing resistant bacteria [3–6], while keeping the bulk structure and main properties of the material

 doi:10.20944/preprints202010.0404.v1

mostly unaltered [7–11]. Silver ions can be easily exchanged with the Na+ ions of the bioactive glass due to their similarities in ionic radius and valence. The penetration power of the silver ions into the glass depends strongly on the reaction conditions. They can be deposited on the surface or penetrate into the glass network. Verne et al. [12] reported on the preparation of silver doped bioactive glass (SiO2-CaO-Na2O) by ion exchange in molten salts and in aqueous solution. The results indicated that in the latter case, silver ions introduced into the glass network and/or on the surface provide better control of the amount of incorporated silver as compared to the Ag-modified materials prepared by the molten salt approach, thus avoiding cytotoxic effects [12]. The main issue related to ion exchange in aqueous solutions relates to the associated long reaction times, lasting from days to months [10,12]. In this regard, sonochemistry has been demonstrated as a suitable approach to reduce mainly bulk high temperatures, high pressures and long reaction times involved in some methods [13]. The production of silver nanoparticles from aqueous silver nitrate solutions sonochemically was investigated by Mănoiu and Aloman [14]. The proposed method consisted in applying a strong flow of ultrasonic energy [14,15] to silver nitrate solutions with concentrations ranging from 0.1M to 0.001M at 30°C for 1h. These conditions led the fluid to cavitate (i.e., formation, growth and implosive collapse of bubbles) [13] providing quasi-spherical silver nanoparticles of about 7 nm average particle size. He et al. [16] reported on the formation of Ag nanoparticles by an ultrasonic approach in acidic, neutral and alkaline aqueous media without using any reductant and surfactant reagent. They proposed that upon sonication of aqueous silver nitrate solution, water molecules decompose to hydrogen and hydroxyl radicals (H· and ·OH, respectively). Finally, H· radicals supply electrons to Ag+ which is reduced to metallic silver [16].

In the present work, silver from AgNO3 solution has been incorporated into the surface of a bioactive glass which contains magnesium, fluorine and features significantly lower sodium content as compared to that of the well-known 45S5 Bioglass® [17–19]. The combination of the ion exchange approach with the ultrasonic treatment has been shown to represent a facile, time-saving method to modify the surface of a bioactive glass with Ag. The structural characterization of the Ag-modified glass samples was performed using X-ray diffraction, UV-Vis spectroscopy, TEM and SEM microscopy before and after exposure of the samples to simulated body fluid for several time spans. The antibacterial activity of silver-containing BG has been assessed using E. coli strain.

2. Materials and Methods

2.1 Preparation of silver-modified glass materials

The bioactive material studied in this work is a glass named BG with the following composition: 4.33Na_2O-30.30CaO–12.99MgO–45.45 SiO_2–2.60P_2O_5–4.33CaF_2 (mol%). It was selected from the series of bioactive glasses designed and developed in the CaO–MgO–SiO_2 system due to beneficial results demonstrated during its application in regenerative biomedicine [17,18,20]. BG glass was produced from powders of technical grade of silicon oxide (purity 99.5%) and calcium carbonate (99.5%) and of reagent grade $4MgCO_3 \cdot Mg(OH)_2 \cdot 5H_2O$, Na_2CO_3, CaF_2, and $NH_4H_2PO_4$ through melting in Pt-crucibles at 1400 ºC for 1 h, in air [17,18,20]. Glass-frits were obtained by quenching of the melts into cold deionized water. Frits were then dried and milled in a high-speed planetary mill (Pulverisette 6, Fritsch, Germany) and sieved to obtain fine particles with sizes below 32 μm. The calculated network connectivity of the BG glass investigated in the present study is about 2.25, which falls into the bioactivity range discussed by Hill et al. [21].

Silver-modified (ABG) glassy materials were prepared by a sonochemical method using fine powders of BG and 0.035 M (0.60 wt.%), 0.077 M (1.25 wt.%), 0.150 M (2.50 wt.%) and 0.220 M (3.70 wt.%) silver nitrate (ACS reagent, ≥ 99.0%, Sigma Aldrich) solutions. The experimental silver modified ABG materials were further denoted as ABG1, ABG2, ABG3 and ABG4, respectively. The solid load of BG powder in the $AgNO_3$ solutions was kept as 10 mg/ml (i.e., 1g of BG was suspended in 100 ml of solution). To avoid photodegradation, the laboratory ware accommodating silver nitrate solutions and ABG glassy materials was covered by aluminum foil. The procedure for ABG glassy

 doi:10.20944/preprints202010.0404.v1

materials preparation is summarized in Scheme 1 and may be described as follows: BG powder was stirred in $AgNO_3$ solutions for 20 min and then a flask with the obtained suspension was placed in the ultrasonic ice-water bath at 35 kHz for 30s. This procedure of sonochemical treatment was repeated 3 times. Then the sonicated suspensions were heat treated at 80°C for 20h in air. After centrifugation, the solid was washed with deionized water and dried at 37°C for 24h.

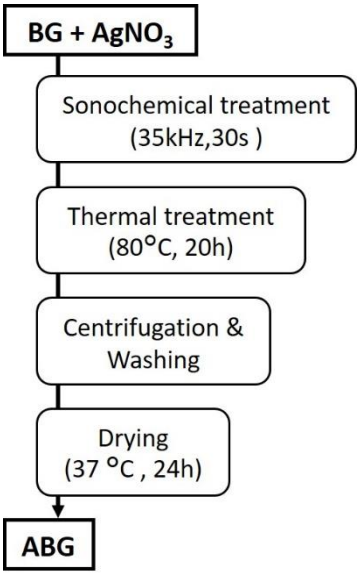

Scheme 1. Proceeding for preparing silver-modified bioactive glass (ABG) materials.

2.2 Physicochemical characterization

The powder X-ray diffraction (XRD) patterns of the as-prepared samples were recorded on a STADI P X-ray diffractometer (STOE&Cie GmbH), equipped with a position-sensitive detector, using Mo Kα (λ = 0.7093 Å) radiation under 45 kV voltage and 30 mA current in the 2θ range of 5-40°. The Fourier transform infrared (FTIR) spectroscopy measurement was performed using a VARIAN 670-IR FTIR spectrometer in the range of 400-4000 cm^{-1}. For this purpose, the samples were mixed with KBr (mass ratio: sample: KBr = 1:150) and pressed into a pellet. The high-resolution transmission electron microscopic (HRTEM) images of the ABG samples were taken with a JEOL JEM 2100F transmission electron microscope. Ultraviolet-visible diffuse reflectance (UV-vis DR) spectra were measured using a Perkin Elmer Lambda 900 UV/VIS/NIR Spectrometer at room temperature. Scanning electron microscopy (SEM) analysis was performed on a Philips XL30 FEG with an acceleration voltage of 10–15 kV.

2.3 In vitro acellular mineralization tests

The in vitro bioactivity of the nanocomposites, reflected in their capability of inducing the mineralization of calcium phosphate phases onto the glass surfaces, was investigated by soaking the as-prepared materials in a protein-free and acellular simulated body fluid (SBF) (75 mg of sample in 50 ml of SBF solution) at 37 °C. The SBF solution was prepared according to the procedure described by Kokubo et al. [22] by dissolving NaCl 8.035 g/L, KCl 0.225 g/L, $K_2HPO_4{\cdot}3H_2O$ 0.231 g/L, $MgCl_2{\cdot}6H_2O$ 0.311 g/L, $CaCl_2$ 0.292 g/L, $NaHCO_3$ 0.355 g/L, and Na_2SO_3 0.072 g/L in distilled water, buffered at pH = 7.4 with 6.118 g/L tris-hydroxymethyl aminomethane and 1 M HCl solution at 37 °C. The ABG nanocomposites were suspended in SBF and sealed in airtight polyethylene flasks. The experiments (static) were performed in an oven at 37 °C for following incubation times: 1 day (1D), 2 days (2D), 3 days (3D), 7days (7D), 12 days (12D), 14 days (14D), 21 days (21D) and 28 days (28D). At the end of each time period, an aliquot was removed from the sample and the solids were separated from the liquid by filtration. The powder was immediately rinsed with deionized water and acetone. The solid powders were characterized by means of FTIR, XRD and SEM. The filtered solution was

 doi:10.20944/preprints202010.0404.v1

collected to determine the ion concentration by inductively coupled plasma optical emission spectroscopy (ICP-OES) analysis. The pH of the solution was also measured. Additionally, ABG4-chitosan composites were prepared and the same SBF test described before for the silver modified glasses was performed. For the preparation of 1 g of ABG4-chitosan composite, 20 mg of chitosan (medium molecular weight, Sigma Aldrich, Germany) were dissolved in aqueous acetic acid. Subsequently, 8.6 mg of ABG4 powder suspended in deionized water were added dropwise, under continuous stirring, to the chitosan solution until a homogeneous composite containing 2wt.% chitosan and 0.86wt.% ABG4 in 0.1M acetic acid was obtained.

2.4 Antibacterial activity

The experiments of bactericidal activity have been performed on TOP10 chemically competent E. coli (Thermo Fisher Scientific). The bacteria were previously chemically transformed and carried a plasmid containing the ampicillin-resistance cassette, to facilitate their handle in non-sterile conditions. They were grown at 37°C in Luria-Bertani medium (LB medium, Sigma) in presence of ampicillin (Sigma, 100 μg/mL) and constantly shaken at 180 RPM.

Two experimental compositions namely ABG3 and ABG4 were sterilized by autoclaving and subsequently added to sterile LB medium (with 100 μg/mL of ampicillin). For comparative purposes the unmodified bioactive glass BG was also tested. Two experiments were performed to investigate the antibacterial activity of the samples:

2.4.1. Analysis of bacterial growth inhibition by contact:

107 bacteria were plated on LB broth agar plates (Sigma) with ampicillin and four areas of the plates were treated with 10 μL of specific BG glass particulates (200 mg/mL). The inhibition of bacterial growth was observed after 24 hours at 37°C.

2.4.2. Analysis of bactericidal action over time:

The experiment was performed in 96-well plates with U-bottom in a total volume of 200 μL, 100 μL of bacteria inoculum (107 bacteria/mL) and 100 μL of glass particulates solution (20 mg/mL). Therefore, the final working concentration of glass particulates was 10 mg/mL. The amount of bacteria was evaluated after 1h, 2h and 4h of incubation at 37°C with the glass particulates. To obtain the colony forming units (CFU), bacteria were vortexed, diluted and plated on LB broth with agar plates (with 100 μg/mL of ampicillin) for 24 hours at 37ºC.

The statistical differences between experimental conditions were calculated according to the Student's T-test of Prism 8 software (Graph Pad). The samples were considered significantly different when the p value was less than 0.05.

3. Results and discussion

3.1. Chemical and microstructural characterization of silver modifed glasses (ABG)

The XRD patterns of the samples investigated within this study are shown in Figure 1a. The XRD patterns indicate that BG is X-ray amorphous, where a broad hump centered at approximately 13° is assigned to the amorphous silica network. The prepared ABG glassy materials are of amorphous nature as well, thus, the reflections with low intensity observed in the XRD patterns may be ascribed to crystalline silver (I, II, and III) oxide phases (Ag_2O, Ag_3O_4, and Ag_3O) [23–25] and elemental silver (Ag) [26]. The presence of elemental Ag was also corroborated by UV-Vis spectroscopy. Figure 1b shows the UV-Vis spectra of the ABG glassy samples prepared using solutions with different concentrations of silver nitrate. Silver nanoparticles (NPs) interact with light strongly due to their known surface plasmon resonance (SPR) [27]. Typically, the SPR peak of the Ag NPs is located

Preprints (www.preprints.org) | NOT PEER-REVIEWED | Posted: 20 October 2020 doi:10.20944/preprints202010.0404.v1

between 390 nm to 476 nm. The absorption bands of the ABG samples are located in the visible range (from ca. 350nm to 550 nm) with the plasmon peak centered at 392 nm. The detection of the SPR peak, which was not present in the parent glass (BG), confirms the presence of the elemental silver in all as-prepared ABG samples [16].

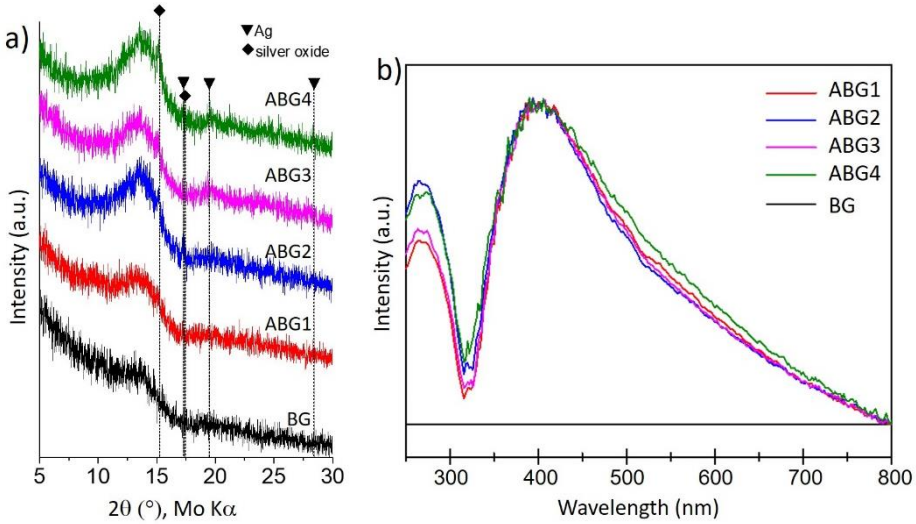

Figure 1. (**a**) X-ray diffraction patterns and; (**b**) UV-Vis spectra of the as-prepared silver modified ABG glassy materials and the parent glass BG (black solid line). Peak centered at 392 nm corresponds to the characteristic SPR peak of silver nanoparticles on the surface of the silver glassy materials. This peak is no detected in the spectrum of the parent glass BG.

The HRTEM image (Figure 2a) reveals the presence of silver nanospheres with an approximate mean diameter of 10 nm. These nanospheres tend to aggregate on the surface of the glass forming silver clusters of different sizes with quasi-spherical shapes (Figure 2b). Some case studies related to the Ag incorporation into the surface of bioglasses reported on the presence of needle-shaped Ag clusters, which were discussed within the context of possibly damaging the cell walls of the bacteria and consequently inhibiting their activity [28]. However, as the silver clusters in the present study are spherical, one may expect that physical damages of the cell walls are rather unlikely.

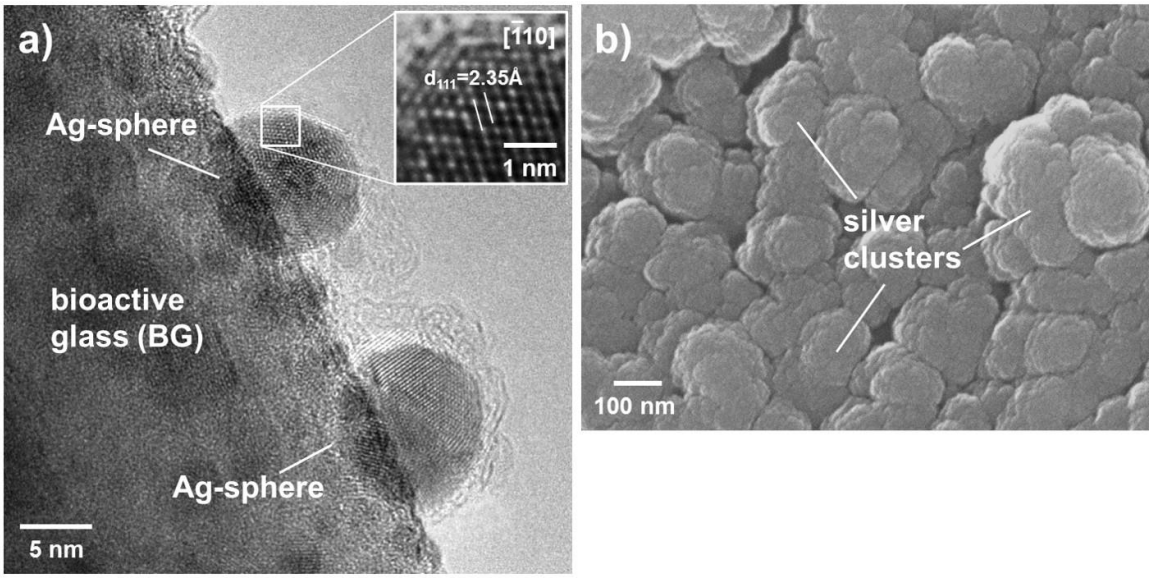

Figure 2. (**a**) HRTEM micrograph of ABG3 showing that the surface of BG is covered by silver nanoparticles of about 10 nm and; (**b**) HR-SEM micrograph of the surface of ABG2.

One question that may arise at this point is regarding the origin of elemental silver. Since neither natural or chemical reductants have been directly used during the preparation of the ABG samples,

 doi:10.20944/preprints202010.0404.v1

most likely, silver nanoparticles were formed during the sonochemical treatment. It is known that the ultrasonic irradiation of the H_2O generates highly reactive species (mainly H· and ·OH) which might be responsible for reducing silver ions to elemental silver [16]. On one hand, according to He el al. [16], the reductive rate of Ag^+ in pure water via ultrasonic irradiation is very low, however, it may be enhanced by increasing the concentration of OH^- in the fluid. It is known that when silicate glasses, like the bioactive glass investigated in the present work, are in contact with water ion exchange reactions between modifiers (such as Na^+, Ca^{2+} and Mg^{2+}) and H^+ from the surrounding fluid take place at the glass/liquid interface leading to a local (near the surface) increase of the concentration of OH^- [29]. $AgNO_3$ in alkaline media forms $Ag(OH)_x$ species in equilibrium with Ag_2O [30,31], whose presence in the silver modified glasses has been shown by X-ray diffraction (Figure 1a). Then, upon performing ultrasonic conditioning Ag_2O crystalline phases are reduced to metallic silver [16]. Contemporarily, that does not exclude the fact that along the procedures involved silver ions may be exchanged with Na+ ions in the upper atomic layers of the BG, as demonstrated by Verne et al. [12].

The mid infrared spectra of the investigated samples, prepared with increasing silver content from 0 to 3.7wt% (Figure 4a), exhibit three broad transmittance bands in the region from 1200 cm^{-1} to 400 cm^{-1} ascribed to the characteristic vibrations of SiO_4 tetrahedron units with different number of bridging oxygen (BO) atoms. The band located at high wavenumbers (from 1200 cm^{-1} to 850 cm^{-1}) is attributed to the Si–O asymmetric stretching mode of the non-bridging oxygens (NBOs) [32,33]. It shows that the network mainly features Q^2 species (SiO_4 sites with 2 BO and 2 NBOs) along with Q^3 groups (SiO_4 sites with 3 BOs and one NBO) [20,34]. The bands between 730 and 800 cm^{-1} are ascribed to bending vibrations of the same units, while the bands between 400 and 550 cm^{-1} may be attributed to rocking motion of Si-O-Si units [20]. The structure of all investigated glasses is similar to that of the parent glass BG, which indicates that the silver treatment performed within this work does not significantly alter the glass network.

3.2. In vitro acellular mineralization assessments of the silver modified glasses

The formation of apatite upon exposure the glasses in SBF as well as the bacteria growth are strongly pH dependent [35]. Thus, pH evolution for BG and for ABG materials in SBF at 37 °C for different periods of time was monitored. The pH of the SBF solution was fixed as 7.4±0.1. As shown in Figure 3, compared to the parent BG, in all ABG glassy materials the pH demonstrated much faster increase, while this tendency was less pronounced after 1 day of immersion. The maximum pH values recorded for the silver modified samples were 8.0±0.1 after 72 hours of immersion (Figure 3). The observed increase about 0.6 pH units is relatively low in contrast with the increase observed for the benchmark 45S5 which rises the pH of the SBF solution above 1 pH units [22]. The lower increment observed might be associated with the fluoride ions that are part of the BG used within this work. While the cations such as Na^+, Ca^{2+} and Mg^{2+} from the glass surface are leached out from the glass to the solution and replaced by H^+, F^- ions are exchanged with OH^- ions, thus depleting the concentration of hydroxide ions in the solution and buffering the effect of alkali/ alkaline earth ions [21]. In spite of that, one can notice that the pH values of the silver modified glasses are always beyond the values gathered for the parent glass. This fact might be associated with the release of silver ions during the first hours of immersion according with the evolution of silver concentration in the fluid over the time (Figure 5f) which will be explained in detail below: silver ions from the surface are exchanged with hydrogen cations from the solution, thus, increasing the concentration of hydroxide anions in the solution. Conversely, the parent BG exhibited lower pH values with a plateau after the first hours of immersion until 2 days of immersion, followed by further decline.

Preprints (www.preprints.org) | NOT PEER-REVIEWED | Posted: 20 October 2020 doi:10.20944/preprints202010.0404.v1

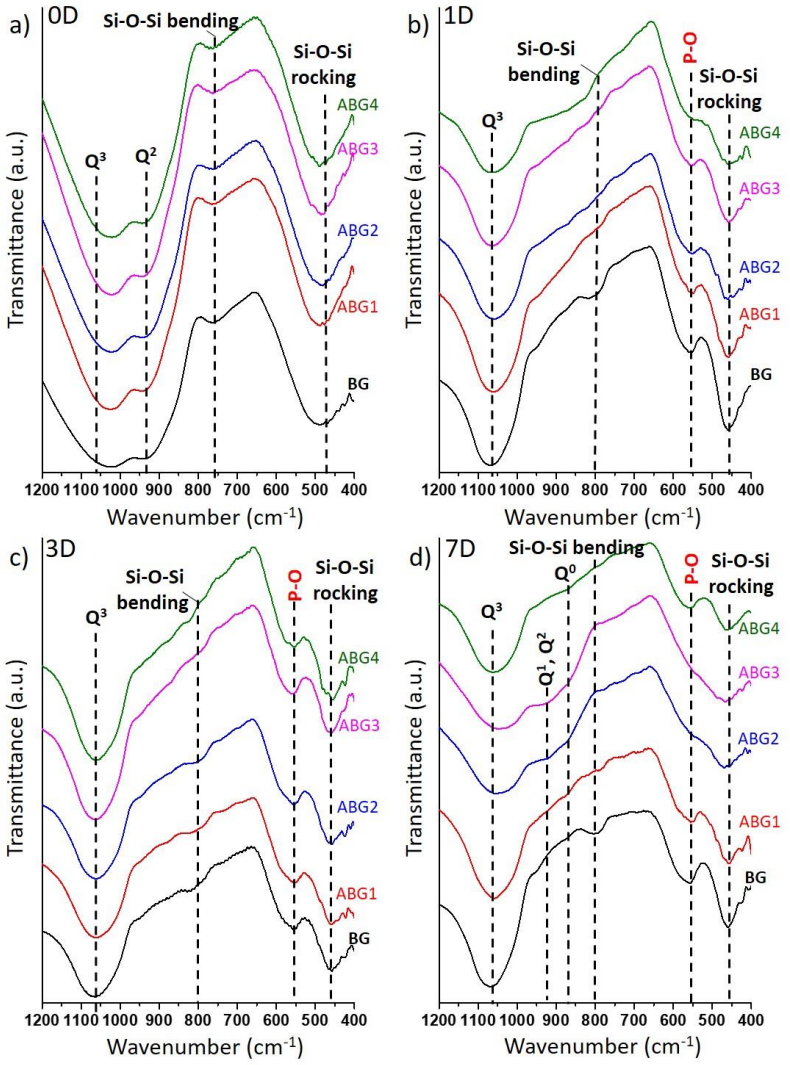

Figure 3. Evolution of pH upon immersing ABG nanocomposites for different time spans.

Figure 4 illustrates mid infrared spectra obtained for the investigated materials upon exposure in SBF for 0 days (0D, Figure 4a), 1day (1D, Figure 4b), 3days (3D, Figure 4c), and 7days (7D, Figure 4d). The spectra of the soaked samples clearly show that the band attributed to Q^2 (SiO4 sites with 2 BO and 2 NBOs) disappeared, while the broad band ascribed to Si-O-Si rocking motions gets narrower. Bands related to the Si–O asymmetric stretching mode of the NBO (namely, Q^2, Q^1, and Q^0) are detected only in the silver modified glasses after exposure in SBF (Figure 4). Moreover, a single peak at ~560 cm^{-1}, ascribed to P–O bending vibrations, can be observed in the spectra of both silver-modified and silver-free glasses from the beginning of the test. Since only a broad single peak is observed it may suggest the presence of amorphous, rather than crystalline, calcium phosphate phases [36].

Preprints (www.preprints.org) | NOT PEER-REVIEWED | Posted: 20 October 2020 doi:10.20944/preprints202010.0404.v1

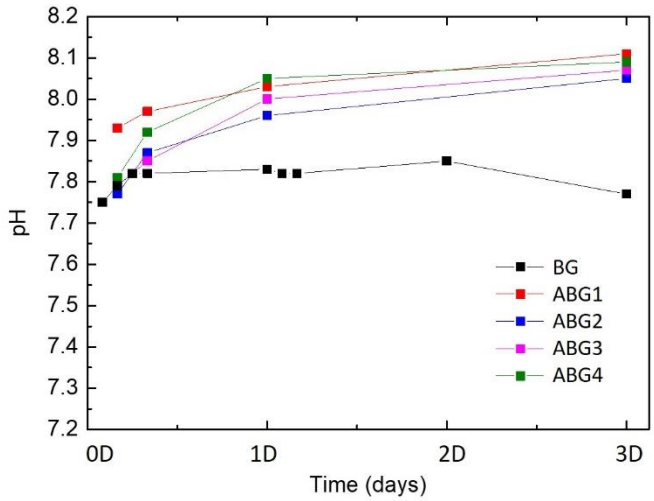

Figure 4. Mid infrared spectra of the ABG1, ABG2, ABG3, and ABG4 glassy materials and parent BG glass upon SBF exposure for (**a**) 0days (0D); (**b**) 1day (1D); (**c**) 3 days (3D); and (**d**) 7days (7D).

The evolution of the ion concentration during the SBF test was assessed by optical emission spectroscopy. The leaching profiles of Si, Na, Ca, Mg, P and Ag are shown in Figure 5. It can be observed that the silicon, sodium, calcium, and magnesium concentrations evolve similarly in both ABG materials and silver-free parent glass during the first week of immersion. However, during the second week of exposure in SBF, the concentration of Si, Na, Ca and Mg increased in the ABG compositions while it was constant (e.g. Mg) or even decreased (e.g. Si, Na, and Ca) in the parent glass.

It is well documented that the removal of phosphorous from SBF solution is attributed to the precipitation of phosphate species on the glass surface. It can be observed that while the parent glass demonstrates a smooth decrease in phosphorus concentration, the ABG samples show more abrupt profiles. Importantly, the Ag leaching profiles in ABG samples (Figure 5f) suggest abrupt growth in Ag ion concentration during the first hours till 1 day of immersion with steady increase in silver concentration along all 12 days of immersions (with the exception revealed for 7 days of immersion in ABG4).

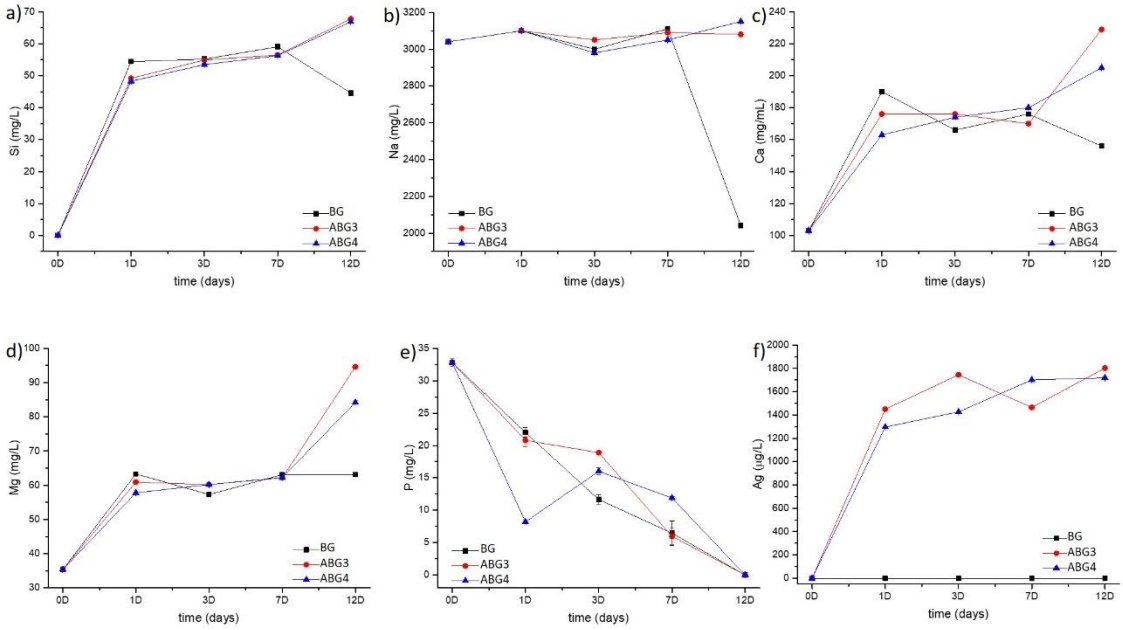

Figure 5. Evolution of the concentration of (**a**) Si; (**b**) Na; (**c**) Ca; (**d**) Mg; (**e**) P; and (**f**) Ag in SBF solution upon immersing ABG nanocomposites for different time spans.

Preprints (www.preprints.org) | NOT PEER-REVIEWED | Posted: 20 October 2020 doi:10.20944/preprints202010.0404.v1

The mineralization of bioactive glasses is typically investigated by the observation of amorphous and crystalline calcium phosphate developed on the glass surface upon immersion in SBF solution. Figure 6a shows XRD patterns of sample ABG4 after immersion in SBF solution for different periods of time that revealed characteristic diffraction peaks of AgCl (ID #: 00-031-1238) [12]. As stated in the literature [12], during the SBF test, ABG4 releases Ag^+ ions which speedily react with the chlorides from the SBF solution leading to the precipitation of insoluble AgCl crystals on the surface of the glass. Moreover, the AgCl crystals on the surface may prevent the direct interaction between glass surface and SBF, thus the release rate of silver ions slows down as can be shown in the evolution of the concentration of silver from 1 days of immersion in the fluid (Figure 5f).

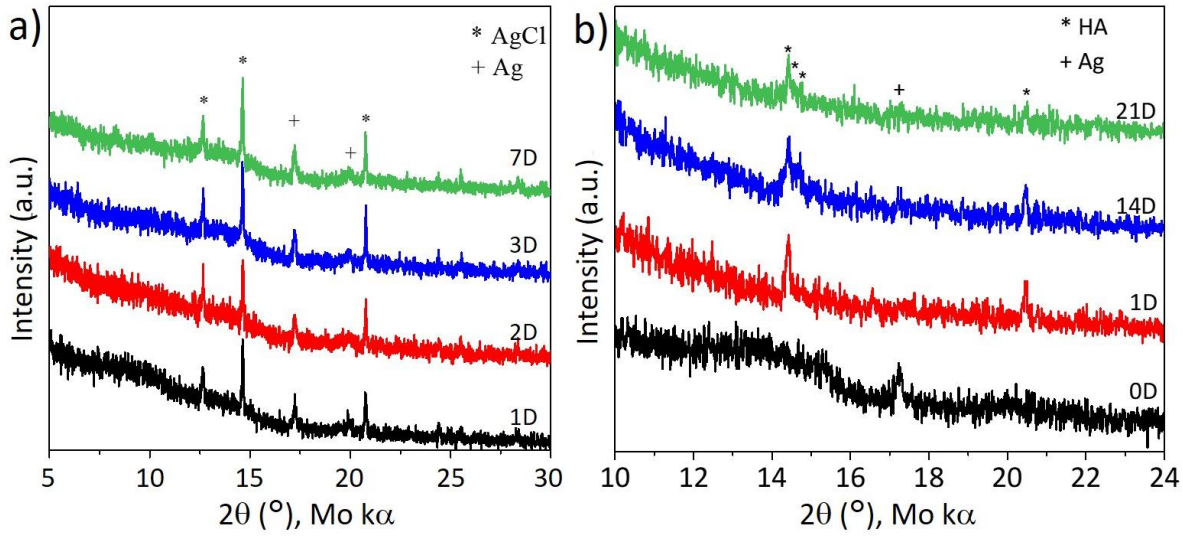

Figure 6. XRD patterns of (**a**) ABG4 as-prepared; and (**b**) ABG4 embedded in 2wt.% chitosan upon exposure in SBF for different periods of time.

However, the SEM micrographs of the as-prepared ABG4 glass upon immersion in SBF for 2 weeks (Figure 7) shown some cauliflower facets characteristic of hydroxyapatite (HA). Then, we may conclude that the most intense diffraction peak of AgCl at 14.69° overlaps with the main peak of HA masking the presence of calcium phosphate crystalline phases.

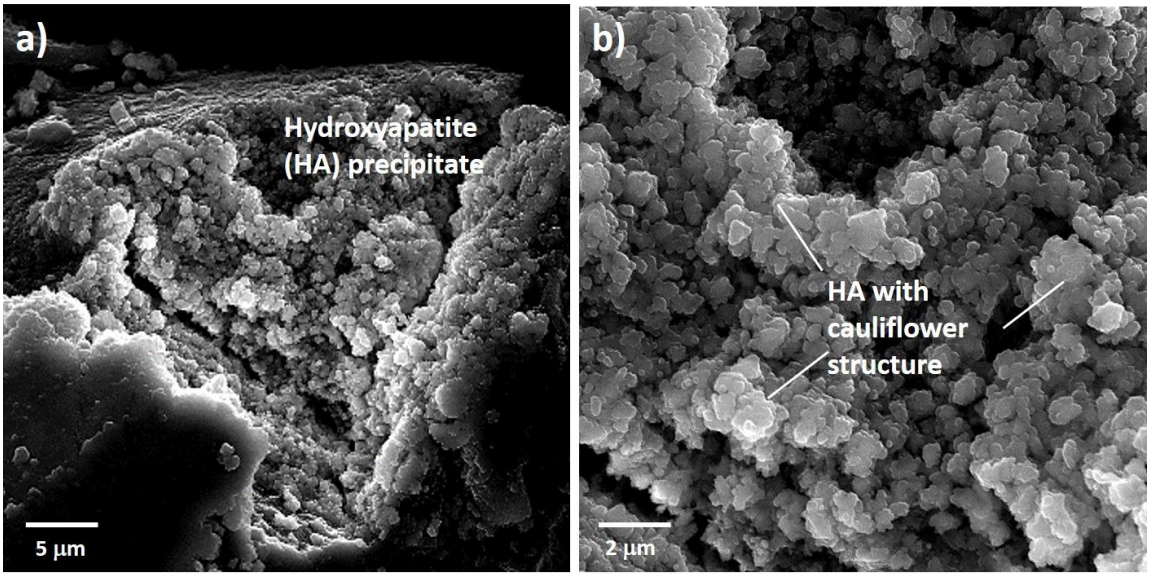

Figure 7. SEM micrographs of ABG4 upon immersion in SBF for 2 weeks at different magnifications.

Preprints (www.preprints.org) | NOT PEER-REVIEWED | Posted: 20 October 2020 doi:10.20944/preprints202010.0404.v1

This issue was partially solved by incorporation of chitosan as a silver chelating agent. It is well established that chitosan as a polysaccharide biopolymer exhibits excellent chelating properties with metals and semiconductors due to the presence of both amino and hydroxyl groups in its monomers [37]. Then, ABG4 glass was embedded in 2 wt.% chitosan [37] and subsequently immersed in SBF for different time spans. The XRD diffraction patterns of the ABG4-BG composite before and after immersion in SBF (for 1D, 14D, and 21D) are shown in Figure 6b. Before immersion in SBF (0D), a weak reflection of Ag was observed at 17.24 ° [38], which disappeared over the first hours. For all immersions lasting longer than 1D, the diffraction patterns showed reflections at 14.40 °, 14.57 °, and 14.77 ° together with intensive amorphous background which can be assigned to the characteristics reflections of hydroxyapatite (HA) [35]. Accordingly, incorporation of chitosan upon SBF testing of silver modified bioactive glass was shown to be an appropriate approach to reaffirm HA crystals formation.

3.3. Bactericidal activity of the as-prepared of the silver modified glasses

To evaluate the bactericidal properties of the silver modified glasses, two different experiments were performed: inhibition of bacterial growth and bactericidal activity. Figure 8a shows the inhibition of bacterial growth in the presence of the silver-containing as well as silver-free bioactive samples. It can be clearly observed that the silver-modified glassy materials (ABG3 and ABG4) inhibited bacterial growth, as revealed by the presence of four clean areas in the respective plates, while the silver-free BG sample shows a uniform bacterial growth. The bactericidal activity of the silver-modified samples over time is depicted in Figure 8a. Samples treated with silver-modified glasses showed a reduction of almost two orders of magnitude in bacterial number after one hour as compared to the silver-free BG sample ($p < 0.05$). Moreover, the number of bacteria treated with silver containing glasses decreased continuously up to reaching the detection limit after ca. 1.5h and ca. 2h for ABG4 and ABG3, respectively. Finally, samples treated with silver-free BG showed a slight decrease of bacterial number after one hour compared with the inoculum. However, after two hours of incubation at 37 °C, the number of bacteria increased to be comparable to the one of the inoculum. After four hours, the number of bacteria was one order of magnitude higher than that of the inoculum, indicating that BG has no bactericidal properties. The decrease of the number of bacteria observed in the silver free sample during the first hours of the analysis may be due to the release of F^- ions [39,40]. In conclusion, the silver-modified ABG glassy materials showed strong bactericidal activity against E. coli, which was not observed in the case of the silver-free parent BG.

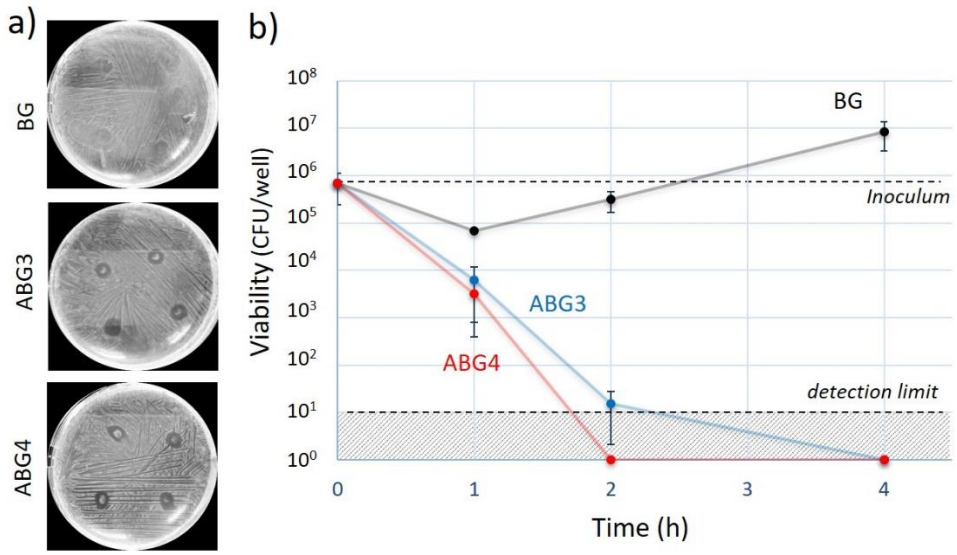

Figure 8. (**a**) Inhibition of bacterial growth in petri dishes by contact with ABG3 and ABG4 samples; and (**b**) bactericidal activity of ABG3 and ABG4 materials in LB broth after 1h, 2h and 4h.

5. Conclusions

The present study demonstrates that silver nanoparticles with sizes lower than 10 nm may be incorporated into the surface of BG glass using a facile, fast, and low-temperature synthesis route. According to the mid infrared spectra, the structure of ABG materials is similar to that of the parent glass BG, which indicates that the treatment performed within this work does not significantly alter the structure of the glass network and thus does not interfere with its bioactivity process mechanisms.

Antibacterial tests showed that the silver-containing glasses, unlike the parent BG, inhibit the growth of E. coli. and exhibit rapid decrease in its viability, reaching the limit of detection after a maximum of 2 hours.

Funding: D.U.T. acknowledges financial support from the Alexander von Humboldt Foundation. E.I. acknowledges funding from the DFG within the Heisenberg program (IO 64/14-1).

Author Contributions: Conceptualization, D.T., I.G. and, E.I.; methodology, D.T., I.G., S.L., F.D.R, and A.F.; software, I.G., F.X, and M.B; validation, I.G., F.X, M.B, F.D.R., and A.F.; formal analysis, I.G., F.X, M.B, and F.D.R.; writing—original draft preparation, I.G.; writing—review and editing, D.T., I.G. and, E.I.; project administration, D.T., I.G. and, E.I.; funding acquisition, I.G., E.I. and R.R. All authors have read and agreed to the published version of the manuscript.

Acknowledgments: The authors thank M. Jamil (Institut für Materialwissenschaft, Technische Universität Darmstadt, Germany) for his assistance in characterizing the nanocomposites as well as C. Scholz (Institut für Geowissenschaften, Ruprecht-Karls-Universität Heidelberg, Germany) for performing ICP-EOS analysis.

Conflicts of Interest: The authors declare no conflict of interest.

References

1. Lu, H.; Liu, Y.; Guo, J.; Wu, H.; Wang, J.; Wu, G. Biomaterials with Antibacterial and Osteoinductive Properties to Repair Infected Bone Defects. *Int. J. Mol. Sci.* **2016**, *17*, 334, doi:10.3390/ijms17030334.
2. van de Belt, H.; Neut, D.; Schenk, W.; van Horn, J.R.; van der Mei, H.C.; Busscher, H.J. Infection of orthopedic implants and the use of antibiotic-loaded bone cements. A review. *Acta Orthop. Scand.* **2001**, *72*, 557–571, doi:10.1080/000164701317268978.
3. Kim, J.S.; Kuk, E.; Yu, K.N.; Kim, J.-H.; Park, S.J.; Lee, H.J.; Kim, S.H.; Park, Y.K.; Park, Y.H.; Hwang, C.-Y.; et al. Antimicrobial effects of silver nanoparticles. *Nanomedicine: NBM* **2007**, *3*, 95–101, doi:10.1016/j.nano.2006.12.001.
4. Chaloupka, K.; Malam, Y.; Seifalian, A.M. Nanosilver as a new generation of nanoproduct in biomedical applications. *Trends Biotechnol.* **2010**, *28*, 580–588, doi:10.1016/j.tibtech.2010.07.006.
5. You, C.; Han, C.; Wang, X.; Zheng, Y.; Li, Q.; Hu, X.; Sun, H. The progress of silver nanoparticles in the antibacterial mechanism, clinical application and cytotoxicity. *Mol. Biol. Rep.* **2012**, *39*, 9193–9201, doi:10.1007/s11033-012-1792-8.
6. Swathy, J.R.; Sankar, M.U.; Chaudhary, A.; Aigal, S.; Anshup; Pradeep, T. Antimicrobial silver: An unprecedented anion effect. *Sci. Rep.-UK* **2014**, *4*, 7161, doi:10.1038/srep07161.
7. Bellantone, M.; Williams, H.D.; Hench, L.L. Broad-spectrum bactericidal activity of Ag2O-doped bioactive glass. *Antimicrob. Agents. Ch.* **2002**, *46*, 1940–1945, doi:10.1128/aac.46.6.1940-1945.2002.
8. Verné, E.; Ferraris, S.; Miola, M.; Fucale, G.; Maina, G.; Martinasso, G.; Canuto, R.A.; Di Nunzio, S.; Vitale-Brovarone, C. Synthesis and characterisation of bioactive and antibacterial glass–ceramic Part 1 – Microstructure, properties and biological behaviour. *Adv Appl. Ceram.* **2008**, *107*, 234–244, doi:10.1179/174367508X306532.
9. Balagna, C.; Vitale-Brovarone, C.; Miola, M.; Verné, E.; Canuto, R.A.; Saracino, S.; Muzio, G.; Fucale, G.; Maina, G. Biocompatibility and Antibacterial Effect of Silver Doped 3D-Glass-Ceramic Scaffolds for Bone Grafting. *J. Biomater. Appl.* **2011**, *25*, 595–617, doi:10.1177/0885328209356603.
10. Negas, T.; Hilfiker, D.; Bartkowski, S. Simple methods to incorporate silver and copper generate antimicrobial glasses and porous glass-bonded ceramics. *Am. Ceram. Soc. Bull.* **2017**, *96*, 26–31.

11. Kaya, S.; Cresswell, M.; Boccaccini, A.R. Mesoporous silica-based bioactive glasses for antibiotic-free antibacterial applications. *Mat. Sci. Eng. C-Mater.* **2018**, *83*, 99–107, doi:10.1016/j.msec.2017.11.003.
12. Vernè, E.; Di Nunzio, S.; Bosetti, M.; Appendino, P.; Vitale Brovarone, C.; Maina, G.; Cannas, M. Surface characterization of silver-doped bioactive glass. *Biomaterials* **2005**, *26*, 5111–5119, doi:10.1016/j.biomaterials.2005.01.038.
13. Xu, H.; Zeiger, B.W.; Suslick, K.S. Sonochemical synthesis of nanomaterials. *Chem. Soc. Rev.* **2013**, *42*, 2555–2567, doi:10.1039/C2CS35282F.
14. A Vasile-Sorin, M.; Noiu, A.; A Aloman, A. Obtaining silver nanoparticles by sonochemical methods. *U.P.B. Sci. Bull. B*, **2010**, *72*, 179-186.
15. Cheng, J.; Yao, S.; Zhang, W.; Zou, Y. Preparation and characterization of silver colloids with different morphologies under ultrasonic field. *Front. Chem.* **2006**, *1*, 418–422, doi:10.1007/s11458-006-0067-0.
16. He, C.; Liu, L.; Fang, Z.; Li, J.; Guo, J.; Wei, J. Formation and characterization of silver nanoparticles in aqueous solution via ultrasonic irradiation. *Ultrason. Sonochem.* **2014**, *21*, 542–548, doi:10.1016/j.ultsonch.2013.09.003.
17. Tulyaganov, D.U.; Agathopoulos, S.; Valerio, P.; Balamurugan, A.; Saranti, A.; Karakassides, M.A.; Ferreira, J.M.F. Synthesis, bioactivity and preliminary biocompatibility studies of glasses in the system CaO-MgO-SiO2-Na2O-P2O5-CaF2. *J. Mater. Sci.-Mater. M.* **2011**, *22*, 217–227, doi:10.1007/s10856-010-4203-5.
18. Tulyaganov, D.U.; Makhkamov, M.E.; Urazbaev, A.; Goel, A.; Ferreira, J.M.F. Synthesis, processing and characterization of a bioactive glass composition for bone regeneration. *Ceram. Int.* **2013**, *39*, 2519–2526, doi:10.1016/j.ceramint.2012.09.011.
19. Gonzalo-Juan, I.; Tulyaganov, D.U.; Balan, C.; Linser, R.; Ferreira, J.M.F.; Riedel, R.; Ionescu, E. Tailoring the viscoelastic properties of injectable biocomposites: A spectroscopic assessment of the interactions between organic carriers and bioactive glass particles. *Mater. Design* **2016**, *97*, 45–50, doi:10.1016/j.matdes.2016.02.085.
20. Agathopoulos, S.; Tulyaganov, D.U.; Ventura, J.M.G.; Kannan, S.; Saranti, A.; Karakassides, M.A.; Ferreira, J.M.F. Structural analysis and devitrification of glasses based on the CaO–MgO–SiO2 system with B2O3, Na2O, CaF2 and P2O5 additives. *J. Non-Cryst. Solids* **2006**, *352*, 322–328, doi:10.1016/j.jnoncrysol.2005.12.003.
21. Hill, R.G.; Brauer, D.S. Predicting the bioactivity of glasses using the network connectivity or split network models. *J. Non-Cryst. Solids* **2011**, *357*, 3884–3887, doi:10.1016/j.jnoncrysol.2011.07.025.
22. Macon, A.L.; Kim, T.B.; Valliant, E.M.; Goetschius, K.; Brow, R.K.; Day, D.E.; Hoppe, A.; Boccaccini, A.R.; Kim, I.Y.; Ohtsuki, C.; et al. A unified in vitro evaluation for apatite-forming ability of bioactive glasses and their variants. *J. Mater. Sci.-Mater. M.* **2015**, *26*, 115, doi:10.1007/s10856-015-5403-9.
23. Norby, P.; Dinnebier, R.; Fitch, A.N. Decomposition of Silver Carbonate; the Crystal Structure of Two High-Temperature Modifications of Ag2CO3. *Inorg. Chem.* **2002**, *41*, 3628–3637, doi:10.1021/ic0111177.
24. Standke, B.; Jansen, M. Ag3O4, the First Silver (II, III) Oxide. *Angew. Chem. Int. Ed. Engl.* **1986**, *25*, 77–78, doi:10.1002/anie.198600771.
25. Beesk, W.; Jones, P.G.; Rumpel, H.; Schwarzmann, E.; Sheldrick, G.M. X-Ray crystal structure of Ag6O2. *J. Chem. Soc., Chem. Commun.* **1981**, 664–665, doi:10.1039/C39810000664.
26. In-Kook Suh; H. Ohta; Y. Waseda. High-temperature thermal expansion of six metallic elements measured by dilatation method and X-ray diffraction. *J. Mater. Sci.* **1988**, *23*, 757-760, doi.org/10.1007/BF01174717
27. Amendola, V.; Bakr, O.M.; Stellacci, F. A Study of the Surface Plasmon Resonance of Silver Nanoparticles by the Discrete Dipole Approximation Method: Effect of Shape, Size, Structure, and Assembly. *Plasmonics* **2010**, *5*, 85–97, doi:10.1007/s11468-009-9120-4.
28. Hu, S.; Chang, J.; Liu, M.; Ning, C. Study on antibacterial effect of 45S5 Bioglass®. *J. Mater. Sci.-Mater. M.* **2009**, *20*, 281–286, doi:10.1007/s10856-008-3564-5.
29. Brauer, D.S. Bioactive Glasses—Structure and Properties. *Angew. Chem. Int. Ed.* **2015**, *54*, 4160–4181, doi:10.1002/anie.201405310.
30. Evanoff, D.D.; Chumanov, G. Size-Controlled Synthesis of Nanoparticles. 1. "Silver-Only" Aqueous Suspensions via Hydrogen Reduction. *J. Phys. Chem. B* **2004**, *108*, 13948–13956, doi:10.1021/jp047565s.
31. Wang, X.; Wu, H.-F.; Kuang, Q.; Huang, R.-B.; Xie, Z.-X.; Zheng, L.-S. Shape-Dependent Antibacterial Activities of Ag2O Polyhedral Particles. *Langmuir* **2010**, *26*, 2774–2778, doi:10.1021/la9028172.
32. Omori, K. Analysis of the Infrared Absorption Spectrum of Diopside. *Am. Mineral.* **1971**, *56*, 1607–1616.
33. Aronne, A.; Sigaev, V.N.; Champagnon, B.; Fanelli, E.; Califano, V.; Usmanova, L.Z.; Pernice, P. The origin of nanostructuring in potassium niobiosilicate glasses by Raman and FTIR spectroscopy. *J. Non-Cryst. Solids* **2005**, *351*, 3610–3618, doi:10.1016/j.jnoncrysol.2005.09.019.

34. Stoch, L.; Środa, M. Infrared spectroscopy in the investigation of oxide glasses structure. *J. Mol. Struct.* **1999**, *511-512*, 77–84, doi:10.1016/S0022-2860(99)00146-5.
35. Begum, S.; Johnson, W.E.; Worthington, T.; Martin, R.A. The influence of pH and fluid dynamics on the antibacterial efficacy of 45S5 Bioglass. *Biomed. Mater.* **2016**, *11*, 15006, doi:10.1088/1748-6041/11/1/015006.
36. Vecstaudza, J.; Gasik, M.; Locs, J. Amorphous calcium phosphate materials: Formation, structure and thermal behaviour. *J. Eur. Ceram. Soc.* **2019**, *39*, 1642–1649, doi:10.1016/j.jeurceramsoc.2018.11.003.
37. Božanić, D.K.; Trandafilović, L.V.; Luyt, A.S.; Djoković, V. 'Green' synthesis and optical properties of silver–chitosan complexes and nanocomposites. *React. Funct. Polym.* **2010**, *70*, 869–873, doi:10.1016/j.reactfunctpolym.2010.08.001.
38. Villars, P.; Cenzual, K. Pearson's Crystal Data-Crystal Structure Database for Inorganic Compounds. ASM International, Materials Park 2010.
39. Marquis, R.E. Antimicrobial actions of fluoride for oral bacteria. *Can. J. Microbiol.* **1995**, *41*, 955–964, doi:10.1139/m95-133.
40. Lellouche, J.; Kahana, E.; Elias, S.; Gedanken, A.; Banin, E. Antibiofilm activity of nanosized magnesium fluoride. *Biomaterials* **2009**, *30*, 5969–5978, doi:10.1016/j.biomaterials.2009.07.037.